



Facile Synthesis and Characterization of Zn₂V₂O₇ Nanoparticles

V. SIVAKUMAR^{1,2}, R. SURESH¹, K. GIRIBABU¹ and V. NARAYANAN^{1,*}

¹Department of Inorganic Chemistry, University of Madras, Guindy Campus, Chennai-600 025, India

²Orchid chemicals and pharmaceuticals limited, Research and development Centre, Chennai-600 119, India

*Corresponding author: Fax: +91 44 22300488; Tel: +91 44 22202793; E-mail: vnnara@yahoo.co.in

Received: 5 October 2013;

Accepted: 17 April 2014;

Published online: 16 September 2014;

AJC-15949

Zinc vanadate (Zn₂V₂O₇) nanoparticles were synthesized by facile thermal decomposition method. The as-synthesized Zn₂V₂O₇ nanoparticles were characterized by X-ray diffraction, Fourier transform infrared spectroscopy, Ultraviolet-visible (DRS-UV-visible) spectroscopy, photoluminescence spectroscopy, scanning electron microscopy and transmission electron microscopy. X-ray diffraction shows that the synthesized sample belongs to Zn₂V₂O₇. FT-IR confirms the formation of Zn-O bond in the sample. UV-visible and photoluminescence studies reveal the optical property of the Zn₂V₂O₇ nanoparticles. The nanobar-like morphology was confirmed by both SEM and TEM analysis.

Keywords: Zinc vanadate, Nanoparticles, XRD pattern, UV-visible spectroscopy.

INTRODUCTION

Nanoparticles are important materials because of their wide range of applications in various fields like catalysis¹, biosensor²⁻⁵, environmental sensor⁶⁻⁸, batteries⁹, photocatalysis¹⁰⁻¹² and data storage devices¹³. Among the various kinds of nanostructured materials, metal vanadate nanoparticles have considerable attention in the field of catalysis¹⁴, cathode materials in batteries¹⁵ and implantable cardiac defibrillators (ICDs)¹⁶ due to their fascinating structures, electronic, optical and magnetic properties¹⁷. For instance, MVO₄ (M = Pr, Er, Gd, Dy and Nd) shows enhanced catalytic performance in the oxidative dehydrogenation of propane¹⁸. Silver vanadium oxide has been used as a cathode material in a primary lithium anode cell due to its good conductivity and high lithium insertion capability¹⁹. Copper vanadate has also been widely used in lithium batteries as the anode material and can be used for rechargeable lithium batteries to yield specific capacity²⁰. Among the various metal vanadate nanoparticles, zinc vanadate nanoparticles, which possess high discharge capacity, superior high-rate capability and safety, have been studied intensively as a promising cathode material for lithium ion batteries in recent years. Several methods have been reported for the synthesis of zinc vanadate nanoparticles, like co-precipitation method, a template-free solution method and hydrothermal method²¹⁻²³. Among these methods, the thermal decomposition method has much attraction because of low cost, less time consumption and good crystallized products with high

homogeneity. It must be indicated that there are several reports about the synthesis and electrochemical properties of nanosized metal vanadates. To the best of our knowledge, there is no report published so far regarding the synthesis of zinc vanadate nanoparticles and their studies for electrochemical sensing applications. Here, we have selected a facile thermal decomposition method for the synthesis of Zn₂V₂O₇ nanoparticles, which can be utilized for sensor applications.

In this paper, we report a facile method to synthesize the zinc vanadate (Zn₂V₂O₇) nanoparticles using a thermal decomposition method. XRD, FT-IR, UV-visible, photoluminescence, HR-SEM, EDS and HR-TEM have been used to characterize the as-synthesized Zn₂V₂O₇ nanoparticles.

EXPERIMENTAL

Ammonium metavanadate (NH₄VO₃), zinc acetate (Zn(CH₃COO)₂·2H₂O), 1-dodecanol, used in this work were of analytical grade, supplied by Sigma-Aldrich and used as received (*i.e.*, without any further purification).

Synthesis of Zn₂V₂O₇ nanoparticles: Zn₂V₂O₇ nanoparticles were synthesized by a facile thermal decomposition method. In a typical synthesis of Zn₂V₂O₇ nanoparticles, ammonium metavanadate (0.1 mmol), zinc acetate (0.1 mmol) and 1 mL of 1-dodecanol were mixed and then calcined at 450 °C for 5 h in a muffle furnace. The obtained Zn₂V₂O₇ nanoparticles were used for further analysis.

Structure of the synthesized nanoparticles was analyzed by a Rich Siefert 3000 diffractometer with CuK_{α1} radiation

($\lambda = 1.5406 \text{ \AA}$). The formation of metal oxygen bond in the sample was analyzed by FT-IR spectroscopy using a Shimadzu FT-IR 8300 series instrument. The UV-visible absorption spectrum was obtained on a CARY 5E UV-visible-NIR spectrophotometer. The morphology of the sample was analyzed by HR-SEM and HR-TEM by using FEI Quanta FEG 200-high resolution scanning electron microscope and FEI TECNAI G2 model T-30 at accelerating voltage of 250 kV, respectively.

RESULTS AND DISCUSSION

Typical XRD pattern of the as-prepared $\text{Zn}_2\text{V}_2\text{O}_7$ nanoparticles is shown in Fig. 1. All the X-ray diffraction peaks can be easily indexed to the $\text{Zn}_2\text{V}_2\text{O}_7$ with the monoclinic structure (JCPDS No. 70-1532). The observed diffraction peaks, 16.7° , 18.9° , 21.4° , 23.5° , 25.9° , 28.7° , 32.4° , 33.8° , 34.9° , 37.7° , 38.5° , 40.8° , 42.32° , 43.93° , 47.8° , 51.5° , 55.2° , 56.5° , 58.0° , 59.0° , 60.9° , 62.4° , 65.6° and 67.5° corresponding to (110), (002), (020), (021), (200), (112), ($\bar{2}$ 21), (220), (130), ($\bar{2}$ 23), (004), ($\bar{3}$ 13), (040), ($\bar{2}$ 24), (042), ($\bar{3}$ 33), ($\bar{3}$ 34), (150), (151), (044), ($\bar{3}$ 35), ($\bar{4}$ 25), ($\bar{5}$ 11) and (333) planes, respectively. Further, the synthesized $\text{Zn}_2\text{V}_2\text{O}_7$ has the lattice parameter value $a = 7.429 \text{ \AA}$, $b = 8.340 \text{ \AA}$, $c = 10.098 \text{ \AA}$. No peaks from other impurity phases have been detected, indicating that the sample is highly pure. The average crystallite size of the $\text{Zn}_2\text{V}_2\text{O}_7$ nanoparticles were calculated as 61 nm using Scherrer formula,

$$D = K\lambda/(\beta \cos \theta).$$

where, K is a shape factor, λ is the wavelength, β is the full width at the half-maximum of the line and θ is the diffraction angle.

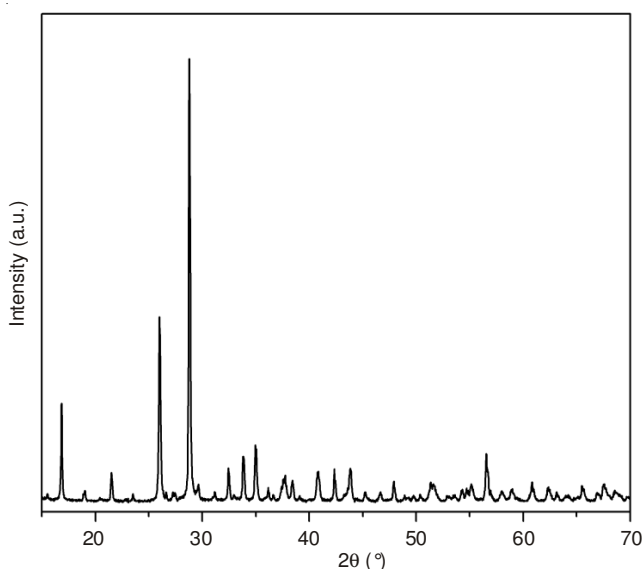


Fig. 1. XRD pattern of $\text{Zn}_2\text{V}_2\text{O}_7$ nanoparticles

FT-IR spectroscopy: Metal oxygen stretching vibration in $\text{Zn}_2\text{V}_2\text{O}_7$ nanoparticles was analyzed by the FTIR spectrum as shown in Fig. 2. The obtained FTIR spectrum of $\text{Zn}_2\text{V}_2\text{O}_7$ nanoparticles is very similar to that reported for $\text{Zn}_2\text{V}_2\text{O}_7$ ²⁵. It shows the bands at 3419, 1631, 1390, 932, 780 and 590 cm^{-1} . The band present at 3419 and 1631 cm^{-1} correspond to the OH stretching vibration and bending vibration of water molecules²⁶.

The band at 932 cm^{-1} is attributed to the VO_3 symmetric stretching vibrations and bands at 932 and 780 cm^{-1} are connected to the VO_3 antisymmetric stretching vibrations²⁷. The band at 590 cm^{-1} is corresponding to the symmetric stretching mode of V-O-V units²⁸. Furthermore, the band observed at 1390 cm^{-1} is caused by overtone band.

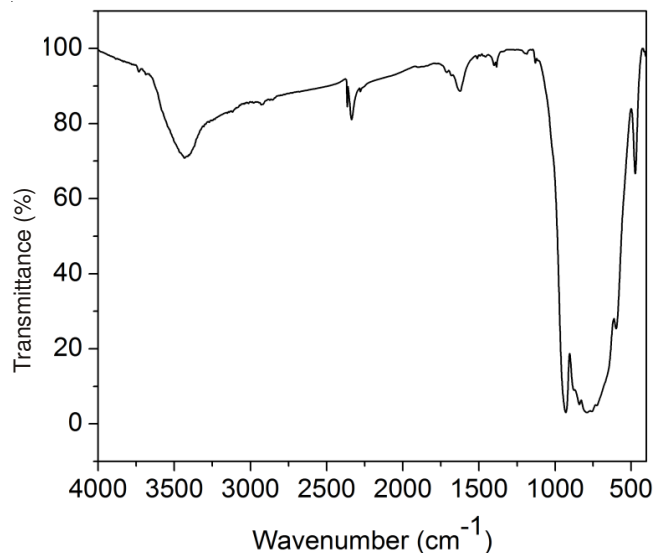


Fig. 2. FT-IR spectrum of $\text{Zn}_2\text{V}_2\text{O}_7$ nanoparticles

UV-visible spectroscopy: UV-visible absorption spectrum of the $\text{Zn}_2\text{V}_2\text{O}_7$ nanoparticles is showed in Fig. 3. The two broad peaks in the range of 300-320 nm and 420-500 nm are due ligand to metal charge transfer band²⁹. The bandgap (E_g) of the nanoparticles can be usually estimated using the classical Tauc equation³⁰, which presents the relationship between the incident photon energy ($h\nu$) and the absorption coefficient (α) near the absorption edge. E_g can be calculated by the following equation as follows:

$$(\alpha h\nu)^n = B(h\nu - E_g) \quad (1)$$

where, $h\nu$ is the photon energy, α is the absorption coefficient, B is a constant relative to the material and n is equal to 2 and 1/2 for a direct transition and indirect transition respectively.

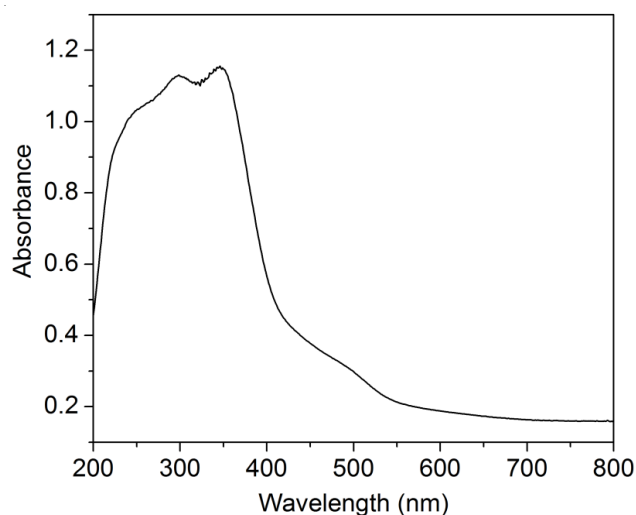


Fig. 3. DRS UV-visible absorption spectrum of $\text{Zn}_2\text{V}_2\text{O}_7$ nanoparticles

The estimated band gap of the synthesized $\text{Zn}_2\text{V}_2\text{O}_7$ nanoparticles is about 2 eV, which is similar to the value reported in literature³¹. Meanwhile, the classic Tauc's approach shows the $\text{Zn}_2\text{V}_2\text{O}_7$ phases with broad bandgap, which may have further applications in nanodevices.

Photoluminescence spectroscopy: Fluorescence property of the $\text{Zn}_2\text{V}_2\text{O}_7$ nanoparticles has been investigated by photoluminescence. The room temperature photoluminescence spectrum of the $\text{Zn}_2\text{V}_2\text{O}_7$ nanoparticles prepared at 450 °C for 5 h exhibits strong blue and green light emission centered at 521 nm and 552 nm, respectively (Fig. 4). Similar results have been observed by Nakajima *et al.* for $\text{M}_2\text{V}_2\text{O}_7$ (M = Ca, Sr and Ba)³². The origin of the blue and green emission bands of $\text{Zn}_2\text{V}_2\text{O}_7$ may be due to the charge transfer transition from O 2p to V 3d orbitals in the VO_4 tetrahedral.

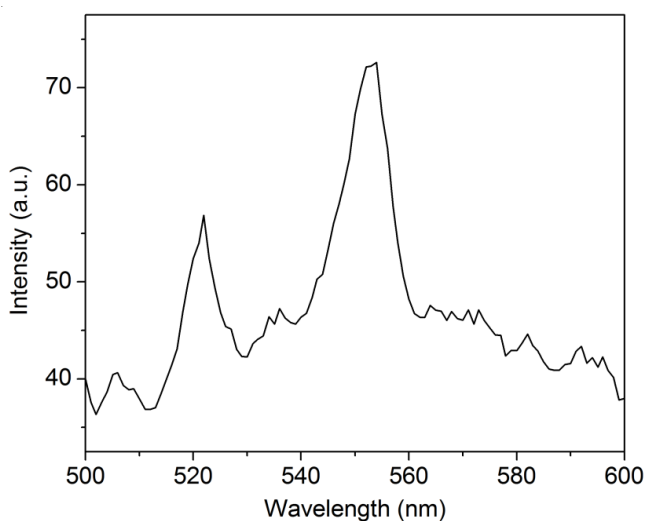


Fig. 4. Photoluminescence emission spectrum of $\text{Zn}_2\text{V}_2\text{O}_7$ nanoparticles

Morphological analysis: Morphology of the as-prepared $\text{Zn}_2\text{V}_2\text{O}_7$ was characterized by SEM and HR-TEM. The SEM image of $\text{Zn}_2\text{V}_2\text{O}_7$ nanoparticles, prepared by calcination of the mixture of NH_3VO_4 and $\text{Zn}(\text{CH}_3\text{COO})_2 \cdot 2\text{H}_2\text{O}$ at 450 °C for 5 h is shown in Fig. 5. It shows that the synthesized product is mostly in agglomerated by sphere-like and irregular particles with the average diameter of about 70 nm.

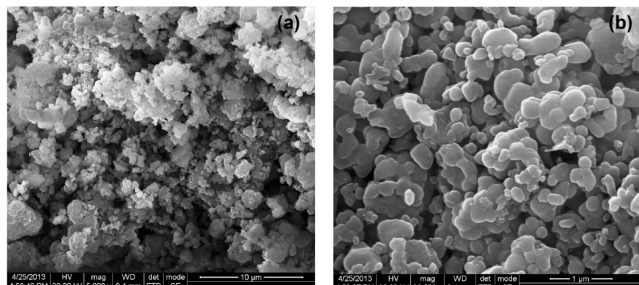


Fig. 5. HR-SEM image of $\text{Zn}_2\text{V}_2\text{O}_7$ nanoparticles (a) magnification at 10 μm and (b) magnification at 1 μm

From the TEM images (Fig. 6), it can be seen that there are spherical and dimensionless particles with pore on their surface which are mainly formed by the release of gaseous product from the interior of the precursor particles.

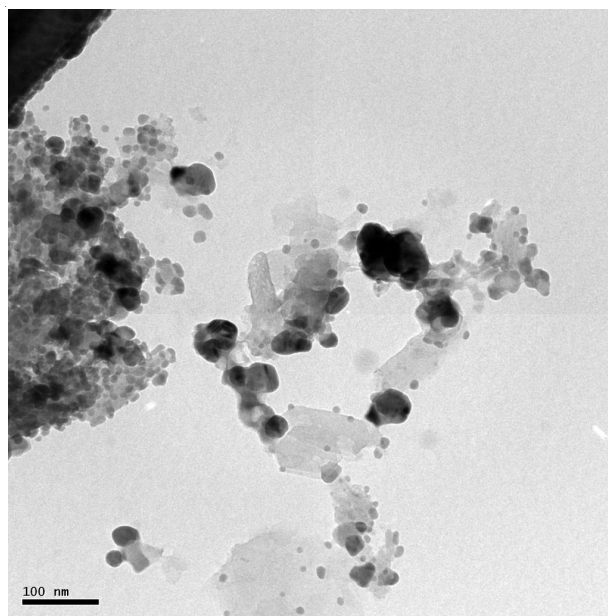


Fig. 6. HR-TEM image of $\text{Zn}_2\text{V}_2\text{O}_7$ nanoparticles

Energy dispersive spectroscopy (EDS) shows that the sample consists of Zn, V and O only (Fig. 7). Further quantitative analysis of EDS finds that the atomic ratio of Zn:V:O is about 2:2:7, indicating that a stoichiometric sample (Zn/V/O = 2 : 2 : 7) is obtained and is consistent with stoichiometric $\text{Zn}_2\text{V}_2\text{O}_7$, which is in agreement with XRD results.

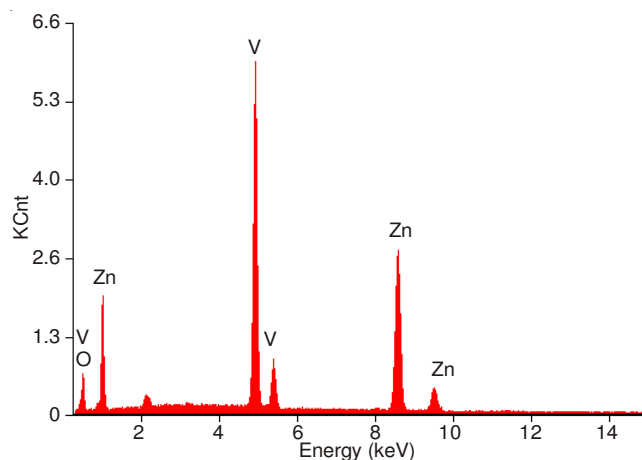


Fig. 7. EDS spectrum of $\text{Zn}_2\text{V}_2\text{O}_7$ nanoparticles

Conclusion

In summary, we demonstrated that the $\text{Zn}_2\text{V}_2\text{O}_7$ nanoparticles can be prepared in high yields through facile thermal decomposition method. The XRD and FTIR spectroscopy confirms the formation of $\text{Zn}_2\text{V}_2\text{O}_7$. The optical absorption property was studied by UV-visible and photoluminescence spectroscopy. The UV-visible spectroscopy reveals that the absorption band at 480 is due to the ligand to metal charge transfer transition. The formation of spherical-like nanoparticles was confirmed by SEM and TEM. The above results show that the synthesized $\text{Zn}_2\text{V}_2\text{O}_7$ nanoparticles could be a better candidate in the field of photocatalysis, batteries and sensors.

ACKNOWLEDGEMENTS

One of the authors (VS) thank Orchid Chemicals and Pharmaceuticals Limited, Chennai. The authors acknowledged the National Centre for Nanoscience and Nanotechnology, University of Madras for providing the HR-TEM facility.

REFERENCES

1. F.F. Bamoharram, *Asian J. Chem.*, **23**, 177 (2011).
2. K. Giribabu, R. Suresh, R. Manigandan, A. Stephen and V. Narayanan, *J. Iran. Chem. Soc.*, **10**, 771 (2013).
3. R. Suresh, R. Prabu, A. Vijayaraj, K. Giribabu, A. Stephen and V. Narayanan, *Mater. Chem. Phys.*, **134**, 590 (2012).
4. R. Suresh, A. Vijayaraj, K. Giribabu, R. Manigandan, R. Prabu, S. Stephen, E. Thirumal and V. Narayanan, *J. Mater. Sci. Mater. Electron.*, **24**, 1256 (2013).
5. R. Suresh, R. Prabu, A. Vijayaraj, K. Giribabu, A. Stephen and V. Narayanan, *Synth. React. Inorg. Metal-Org. Nano-Met. Chem.*, **42**, 303 (2012).
6. K. Giribabu, R. Suresh, R. Manigandan, S. Munusamy, S.P. Kumar, S. Muthamizh and V. Narayanan, *Analyst*, **138**, 5811 (2013).
7. V. Thatshanamoorthy and V. Narayanan, *Asian J. Chem.*, **25**, 6083 (2013).
8. K. Giribabu, R. Suresh, R. Manigandan, L. Vijayalakshmi, A. Stephen and V. Narayanan, *AIP Conf. Proc.*, **1512**, 400 (2013).
9. H. Goktepe, H. Sahan and S. Patat, *Asian J. Chem.*, **21**, 3186 (2009).
10. R. Suresh, K. Giribabu, L. Vijayalakshmi, A. Stephen and V. Narayanan, *AIP Conf. Proc.*, **1447**, 351 (2012).
11. K. Giribabu, R. Suresh, R. Manigandan, A. Vijayaraj, R. Prabu and V. Narayanan, *Bull. Korean Chem. Soc.*, **33**, 2910 (2012).
12. G. Liu, *Asian J. Chem.*, **24**, 1167 (2012).
13. J. Ensling, P. Gutlich, R. Klinger, W. Meisel, H. Jachow and H. Schwab, *Hyperfine Interact.*, **111**, 143 (1998).
14. V. Conte and B. Floris, *Dalton Trans.*, **40**, 1419 (2011).
15. L.Q. Mai, L. Xu, C.H. Han, X. Xu, Y.Z. Luo, S.Y. Zhao and Y.L. Zhao, *Nano Lett.*, **10**, 4750 (2010).
16. A.M. Crespi, S.K. Somdahl, C.L. Schmidt and P.M. Skarstad, *J. Power Sources*, **96**, 33 (2001).
17. M. Machida, Y. Miyazaki, Y. Matsunaga and K. Ikeue, *Chem. Commun.*, **47**, 9591 (2011).
18. C.T. Au and W.D. Zhang, *J. Chem. Soc., Faraday Trans.*, **93**, 1195 (1997).
19. K.J. Takeuchi, A.C. Marschilok, S.M. Davis, R.A. Leising and E.S. Takeuchi, *Coord. Chem. Rev.*, **219**, 283 (2001).
20. M. Morcrette, P. Martin, P. Rozier, H. Vezin, F. Chevallier, L. Laffont, P. Poizot and J.M. Tarascon, *Chem. Mater.*, **17**, 418 (2005).
21. X.J. Sun, J.W. Wang, Y. Xing, Y. Zhao, X.C. Liu, B. Liu and S.Y. Hou, *CrystEngComm*, **13**, 367 (2010).
22. S.Y. Zhang, L.J. Ci and H.R. Liu, *J. Phys. Chem. C*, **113**, 8624 (2009).
23. Y.J. Wei, K.W. Nam, G. Chen, C.W. Ryu and K.B. Kim, *Solid State Ion.*, **176**, 2243 (2005).
24. Y. Liang, P. Liu, H.B. Li and G.W. Yang, *CrystEngComm*, **14**, 3291 (2012).
25. L.Z. Pei, Y.Q. Pei, Y.K. Xie, C.Z. Yuan, D.K. Li and Q.F. Zhang, *CrystEngComm*, **14**, 4262 (2012).
26. H. Hsiang and F.S. Yen, *Ceram. Int.*, **29**, 1 (2003).
27. R.L. Frost, S.J. Palmer, J. Cejka, J. Sejkora, J. Plasil, S. Bahfenne and E.C. Keeffe, *J. Raman Spectrosc.*, **42**, 2042 (2011).
28. R.L. Frost, K.L. Erickson, M.L. Weier and O. Carmody, *Spectrochim. Acta A*, **61**, 829 (2005).
29. N. Gharbi, C. Sanchez, J. Livage, J. Lemerle, L. Nejem and J. Lefebvre, *Inorg. Chem.*, **21**, 2758 (1982).
30. D.L. Wood and J. Tauc, *Phys. Rev., B, Solid State*, **5**, 3144 (1972).
31. A.H. Abdullah, C.Y. Jong and R. Irmawati, *Asian J. Chem.*, **24**, 1627 (2012).
32. T. Nakajima, M. Isobe, T. Tsuchiya, Y. Ueda and T. Manabe, *Opt. Mater.*, **32**, 1618 (2010).